Title
MATRIX ISOLATION STUDIES: MODEL FOR STATIC AND DYNAMIC MATRIX SHIFTS

Author
Chang, Chin-An.

Publication Date
1971-09-01

Submitted to Journal
of Chemical Physics

LBL-173
Preprint

MATRIX ISOLATION STUDIES: MODEL FOR STATIC AND DYNAMIC MATRIX SHIFTS

Chin-An Chang

September 1971

AEC Contract No. W-7405-eng-48

DISCLAIMER

Matrix Isolation Studies: Model for Static and Dynamic Matrix Shifts

Chin-An Chang*

Inorganic Materials Research Division, Lawrence Berkeley Laboratory,

and Department of Chemistry; University of California

Berkeley, California 94720

Abstract

The experimental spectra of Pb in rare gas matrices are correlated with some model calculations. A method is demonstrated to approximate the gas phase transition frequency, ν_{gas}, from those observed in Xe and Kr matrices. Pb and many other metal spectra in the literature are tested. The results show that very good agreement is achieved for the atoms with $s \leftarrow p$ resonance transitions, while too low a calculated ν_{gas} is obtained for the atoms with $p \leftarrow s$ resonance transitions.

The present theories on the matrix shifts are discussed and their predicted dynamic matrix effects compared with observations. It is shown that none of the present theories accounts for the observed dynamic matrix effect. A model is proposed to account for the dynamic matrix effect as well as most of the static matrix effects for many trapped metal atomic spectra.

* Present address: Department of Chemistry
Texas A&M University
College Station, Texas 77843

Introduction

The spectra of atoms in rare gas matrices show[1,2] both static and dynamic matrix effects. The static matrix effects included frequency shifts, appearance of multiplet structures and broadening of the spectral lines. The dynamic effect refers to the different temperature dependences of the multiplet components. For most atoms involving $p \leftarrow s$ transitions, the component highest in frequency in the triplet shifted reversibly to the blue, while the two lower frequency components reversibly shifted to the red when the matrix was warmed up. Examples are Cu,[2] Ag,[2] Li,[3] Na,[4] Ag,[5], Ca,[6] Cd,[6] and Mg.[6]

McCarty and Robinson[7] suggested that the observed frequency shift was due to the interaction of the trapped species with the matrix environment. The observed triplet for Hg and Na in the matrices was attributed to the removal of the three-fold degeneracy of the P state by a John-Teller distortion of the matrix.

Brith and Schnepp[8] studied the multiplet structure of Mn spectrum in Ar by calculating the splitting energy quantum mechanically. Using either a distorted neighbor or missing-neighbor model for the trapping site geometries, they obtained the right order of magnitude of the splitting energies, but only a doublet could be expected from these two models.

Andrews and Pimentel[3] suggested the possible roles of nonnearest neighbor metal-metal interactions in determining the multiplet structure and the splitting energies. Rough agreement with the experiment was obtained.

Brewer and King[9,10] co-deposited Au and Ag in Kr matrix. The mixed metal matrix spectrum showed two triplets corresponding respectively to those of pure Au and Ag in Kr matrix. All the components had the same frequencies as in the pure metal spectra, with the same relative intensities and half-widths, and no extra features appeared. This work seemed to oppose the metal-metal interaction mechanism as being the cause of the multiplet structures.

Meyer and coworkers[2] and Brewer and coworkers[5,9] also studied the spectra of Cu, Ag and Au in Xe, Kr and Ar matrices. The observed triplet for all three metals in the matrices had two components close in frequency to that of the gas phase $^2P_{3/2} \leftarrow {}^2S_{1/2}$, and one to $^2P_{1/2} \leftarrow {}^2S_{1/2}$ transitions. Because there are wide separations in energy between these two gas phase transitions of Cu, Ag and Au, and because the $^2P_{3/2}$ and $^2P_{1/2}$ states split under Stark effect into two and one states, respectively, it was suggested [2,5] that the observed triplet could be due to Stark splittings by the matrix field.

Recently McCarty[11] proposed an explanation for the observed triplet of Hg in the matrices. One line was attributed to the completely isolated Hg atoms, and the other two lines due to resonance interaction between two Hg atoms being nearest neighbors to each other.

It is recalled that there were static as well as dynamic matrix effects. Any satisfactory model for the origin of the multiplet structures in the matrices must account for both of these matrix effects. As is shown later in this paper, none of the earlier theories could explain the observed dynamic matrix effects. Therefore a new model is proposed to account for the dynamic matrix effect as well as most of the static matrix effects observed for the trapped metal atomic spectra.

A. Matrix Effect on the Pb $^3P_1 \leftarrow {}^3P_0$ Absorption Line

As was reported in paper I, the single strong line of the Pb absorption spectra observed in rare gas matrices was assigned to the Pb 6p7s $^3P_1 \leftarrow 6p^2\ ^3P_0$ transition. This line had a half-width of about 400 cm^{-1}, and was blue-shifted from the gas phase value by several thousand cm^{-1}. On warming the matrices, a reversible red shift was observed. The last fact suggested that the absorption frequency of Pb could be closely related to the interaction between Pb atom and the surrounding matrix atoms. This was based on the facts that (1) the rare gas crystals expand reversibly as the temperature is increased,[12,13] and (2) as in the pressure effect studies of the alkali metal atoms,[14] the rare gas atoms were expected to interact differently with the ground and excited states of Pb atom; the net difference between these two interactions could then give rise to the observed frequency shift in the matrices. To test this possible mechanism, calculations were carried out using the Lennard-Jones 6-12 potential described by McCarty and Robinson.[7]

McCarty and Robinson used the Lennard-Jones 6-12 potential in the form

$$\nu_{ab} = 4\,\epsilon_{ab}[12.13(\sigma_{ab}/d_{ab})^{12} - 14.45(\sigma_{ab}/d_{ab})^{6}] \qquad (1)$$

where σ_{ab} is the distance between species a and b at which the attractive force balances the repulsive one. McCarty and Robinson then made the assumption

$$\epsilon_{ab}\sigma_{ab}^{6} \approx (\epsilon_a\sigma_a^{6})^{\frac{1}{2}}(\epsilon_b\sigma_b^{6})^{\frac{1}{2}} .$$

Two equations of form (1) were needed, one for each of the ground and excited states of the trapped species while the matrix atoms remained in their ground state.

After substituting the known values and rearrangement, the equations to be used had the forms

$$\text{for Pb/Xe} \qquad \Delta\nu_{ab} d_{ab}^{6}/45420 \approx (52.7/d_{ab}^{6})\ \Delta_{12} - \Delta_{6} \tag{2}$$

$$\text{for Pb/Kr} \qquad \Delta\nu_{ab} d_{ab}^{6}/28333 \approx (39.2/d_{ab}^{6})\ \Delta_{12} - \Delta_{6} \tag{3}$$

$$\text{where} \qquad \Delta_{12} \equiv (\epsilon_b' \sigma_b'^{12})^{\frac{1}{2}} - (\epsilon_b'' \sigma_b''^{12})^{\frac{1}{2}}, \text{ etc.}$$

The excited and ground states of Pb atom are denoted by single and double prime, respectively. Using the observed frequency shifts of Pb in Xe and Kr at 20°K, Δ_6 and Δ_{12} were found to be -65.9 $cm^{-\frac{1}{2}} A^3$ and 3.796×10^4 $cm^{-\frac{1}{2}} A^6$, respectively.

After substituting the values of Δ_6 and Δ_{12}, the only variable left in Eqs. (2) and (3) that could affect the $\Delta\nu$ values observed was d_{ab}. These two equations were used to calculate the $\Delta\nu$'s at temperatures above 20°K. The d_{ab}'s needed at each temperature were assumed to be the same as the lattice constants of Xe and Kr at that temperature.[12] It was assumed that the trapped species was at the substitutional site in the matrix gas crystal lattice.

The calculated $\Delta\nu$'s in Xe and Kr at various temperatures are shown in Table I, along with the observed values. Clearer comparisons are shown in Figs. 1 and 2.

The calculated $\Delta\nu$ values in Xe are parallel to and slightly larger than the observed ones at all temperatures investigated. This means that, on warming the matrix, the Pb $^3P_1 \leftarrow {}^3P_0$ line decreases faster in frequency than predicted from the model calculation. The opposite was found for Pb/Kr, however. The Pb line in Kr showed a smaller red shift at higher temperatures compared to the predicted values. When the same set of Δ_6 and Δ_{12} obtained above was applied to Pb/Ar, the calculated $\Delta\nu$ at 20°K was 4017 cm^{-1}, compared to the observed value 5553 cm^{-1}. The failure in the Ar case as well as the negative deviation in Kr are explained later using our new model for the matrix effects.

It is interesting to see how the correlation worked in the 10% Xe-90% Kr matrix. In paper I this matrix was approximated to be composed of eight Xe atoms and four Kr atoms around each Pb atom trapped. The results are shown in Table II. The agreement at higher temperatures was fairly good which could be due to a balancing between the two opposite effects observed in Xe and in Kr matrices.

As Table I shows, the agreement between calculated and observed $\Delta\nu$'s becomes poor only at the highest temperatures. Therefore it was interesting to see whether one could apply this method to other metals to check for the assignment of the lines observed. In other words, the observed frequencies at 20°K in Xe and Kr would be used to calculate the corresponding gas phase frequencies.

It is recalled that in Eqs. (2) and (3) Δ_6 and Δ_{12} could be evaluated if the $\Delta\nu$'s were known, with $\Delta\nu \equiv \nu_{obs} - \nu_{gas}$, where ν_{gas} is the corresponding gas phase transition frequency. According to what was

stated in the last paragraph, ν_{gas} is now treated as an unknown and solved using the ν_{obs}'s in the matrices. There are three unknowns, ν_{gas}, Δ_6 and Δ_{12}; therefore one more equation of similar type is needed. This could be another equation containing Ar as the matrix gas. However, since the deviation between calculated and observed $\Delta\nu$'s in Ar at 20°K was very large, this could not serve the purpose, and an alternative way was used as described below.

The interactions between the matrix atoms and different metal atoms all have one thing in common, i.e., the interaction magnitudes fall off toward zero at infinite separation of the two interacting species. In real cases, one can always find a limiting r beyond which the interaction becomes negligible. This principle is used for the observed spectra frequency shifts in the matrices. The earlier work on Pb indicated that interactions between Pb and the matrix atoms could be well treated with the L-J 6-12 potential. If the same relation between Δ_6 and Δ_{12} as for Pb also held for the other atoms, one additional equation could be constructed to approximate the ν_{gas} values of these metals. Using the Pb frequencies observed, it was calculated that in Xe, $\Delta\nu$ = 3.08 cm^{-1} and 0.047 cm^{-1} at r = 10 Å and 20 Å, respectively. The latter was chosen as the limiting r.

The third equation thus obtained had the form

$$(0.047)(20)^6/45420 \approx 52.7/(20)^6\,\Delta_{12} - \Delta_6 \qquad (4)$$

and the calculated ν_{gas}'s for the various metals using their observed frequencies in Xe and Kr[9,15,16] are shown in Table III.

Pb and Bi were very well treated by this method while the calculated ν_{gas} values of all other metals with p ← s transitions were too low compared to their gas phase values. The different behaviors of these metals from Pb and Bi was attributed to the directional sensitivity of the excited p orbitals involved in these metals when there was an accompanying large increase in orbital size during the electronic excitation. The individual p orbital interacted with strong orientational dependence and could not be treated as point dipoles. The use of L-J 6-12 potential for these atoms was therefore no longer justified as for a spherical electronic distribution like the excited states of Pb and Bi.

Although the method of locating ν_{gas} worked well for Pb and Bi, it did not work at all for the metals with p ← s transition. This might serve as an example that one should be cautious in using the calculated values when an excited p electron is involved in the L-J type calculations.

B. The Predicted Dynamic Matrix Effect From the Earlier Theories

It was pointed out in the Introduction that the earlier theories interpreted the observed multiplet structures by considering only the static matrix effects. The observed dynamic matrix effect, however, must be closely related to the real cause of the multiplet structures observed. Any model proposed for the multiplet structures must also be able to predict correctly the observed different temperature dependences of the multiplet components. The earlier theories are now checked individually in this respect.

Brith and Schnepp[8] proposed a missing-neighbor or distortion model to explain the observed triplet of Mn in Ar. The missing-neighbor model cannot give a reversible frequency shift of the lines observed, irrespective of the shift directions. The warm-up process would anneal the matrix film and fill the vacancies in the neighborhood of the trapped Mn. This would cause disappearance of two of the triplet components on cooling back, in contradiction to the observed reversible shift. The distortion model, although giving the right order of magnitude of the splitting energies, predicts only two lines instead of three.

Andrews and Pimental[3] suggested the role of nonnearest metal neighbor interaction in the appearance of multiplet structures of Li in the matrices. If one assumes no mobility of the metal atoms at higher temperatures, i.e., the distances between the Li atoms remain the same, all multiplet components should not show any frequency shift on warming up the matrix. On the other hand, if the metal atoms move while the matrix film expands with increasing temperature, the metal atoms are expected to move toward one another because of the attractions among them at the distances they are separated, as proposed by the authors. This would give blue shifts for all components according to the potential curves they used. Also, it is doubtful that on cooling back the Li atoms would move back to their original positions against the attractive force among them.

Stark splitting has been suggested[2,5,9] as a possible cause of the triplet structures of Au, Ag and Cu in the matrices. In order to check this model for its predicted temperature dependencies of the triplet components, one has to go into some detail about the nature of the Stark

splitting. This is discussed in the Appendix. Here it suffices to mention that this model also fails to predict the correct temperature dependencies observed.

McCarty[11] discussed the Hg triplet spectra in the matrices. One component is attributed to the completely isolated Hg atoms, and two to the two Hg atoms being nearest neighbors to each other. Let us apply this model to the observed triplet of other metal atoms, M. On warming up, the line due to isolated M atoms would give a red shift due to crystal expansion, while the other two lines would also shift to the red if the two M atoms remain the same distance apart. Even if these two M atoms do move closer yet without forming a M_2 molecule, the two lines they give rise to should show the same sign of frequency shift.

None of these theories accounted satisfactorily for the observed frequency shifts of those metals in the matrices. Therefore, a different approach is taken to try to solve this problem.

C. Model for the Dynamic Matrix Effect

The problem is tackled by considering the formation and structure of the matrix thin films. For a pure rare gas thin film, all the atoms are identical, the main factor determining the structure of the film is the mobility of the atoms on the target. This is determined by the vapor temperature, target temperature, deposit rate and the attractions among the gas atoms. If the first three are kept constant, the mobilities on the target among different gases will depend on their melting points T_m relative to the target temperature.[17] Chopra[18] reported that metal films,

when deposited at or below the temperature of $\frac{1}{3}T_m$, have disordered or amorphous structure. This $\frac{1}{3}T_m$ can therefore be treated as the annealing temperature for the individual metal films. Rare gas atoms are similar to many metal atoms in that they are single atoms and spherical like; the deposited film structure is therefore not complicated by the orientational problems of many molecules. For the matrix-trapped alkali metals,[4] multiple trapping sites were formed because the deposit temperature was too low (4°K) for the matrix gases. After annealing at a higher temperature, the spectra corresponded to those metal atoms in the "abnormal" site disappeared, while the main spectra remained. For the Pb spectra, since the films were deposited at 20°K and the spectrum persisted after annealing, conclusions could be drawn about the stability of the trapping site formed at 20°K.

When the metal vapor is co-condensed on the target with the matrix gas, the much higher T_m of the metal greatly reduces its mobility on the target. Because of this, it is not unreasonable to expect that each metal atom is not in the center of the substitutional site, but penetrates to a certain extent toward the inner layer matrix atoms. If there is further asymmetry in the other two directions (the two mutually perpendicular directions both parallel to the target surface), this can completely destroy the three-fold degeneracy of the p orbitals. The p orbital which is normal to the target suffers greatest distortion and accounts for the highest frequency line in the triplet. On warming up the matrix, the metal atom cannot obtain the same mobility as the rare gas atoms because of its high T_m. The mobility of the metal is therefore negligible compared

to that of the matrix gas atoms. The matrix film will expand three-dimensionally on warming up. However, because of the blocking effect of the target, the normal-to-target direction expansion will be completely outward from the target. This increases the distortion between the metal atom and the inner layer matrix gas atoms and causes a blue shift of the transition line. The other two directions, however, expand without being blocked. This lowers the energies in these two directions and causes red shifts for both. On cooling back, the reverse takes place.

It is emphasized that in the p ← s transitions the ground state is spherically symmetric while the upper state is strongly orientation-sensitive because of the three p orbitals involved that are mutually perpendicular to one another. It is this strong orientation sensitivity toward the matrix environment that causes that splitting when the symmetry is removed.

The Pb work in paper I indicated that only one strong line was observed in all rare gas matrices that could be assigned to the $6p7s\ ^3P_1 \leftarrow 6p^2\ ^3P_0$ transition. This is also expected from the proposed model. The $^3P_1$ state consists of one 6p and one 7s electrons. The 7s electron has a larger orbital size than that of a 6p electron. Therefore, in the excited state, the 7s electron is expected to interact with the matrix environment much more strongly than the 6p electron which lies in an inner orbital. The 6p electron could be in one of the three sublevels of the 6p state, giving rise to three-fold degeneracy. The penetration of the Pb atom toward the inner layer would affect this degeneracy.

But the net difference among the interactions involving the 6p electrons with the matrix environment is expected to be small due to the much larger interaction involving the 7s electron. Therefore, the excited state has only negligible splitting and is included in the breadth of the absorption line. The ground state contains two 6p electrons and is also three fold degenerate. The penetration again destroys this degeneracy, but one expects only a small difference in energy among the three non-degenerate states created. Again this only shows up in broadening the absorption line. Because the 7s orbital has a spherical structure and interacts with matrix environment much more strongly than the inner 6p electron, the net absorption from $6p^2\ ^3P_0$ state to $6p7s\ ^3P_1$ state gives one single line. The breadth of this line is therefore expected to be twice or more than those of the triplet components for the metals with $p \leftarrow s$ transitions. This agreed with the observations.

It is interesting to recall Duley's matrix work on Bi.[15] One strong absorption line was observed at 35 971, 36 363 and 38 610 cm^{-1} in Xe, Kr and Ar, respectively. They were assigned to the $6p^2 7s\ ^4S_{\frac{1}{2}} \leftarrow 6p^3\ ^4S_{\frac{3}{2}}$ transition which was at 32 605 cm^{-1} in the gas phase. Upon warming the matrix, a large shift of this line to lower frequencies was observed. Here the excited state was also spherically symmetric like, similar to the Pb 6p7s state. Apparently the same idea above for Pb could be applied to explain the observed single, strong line of Bi in the matrices.

D. Comparison Between Observed and Predicted Multiplet Structures Using fcc and hcp Trapping Site Geometries

Pure Xe, Kr, Ar and Ne were found to crystallize into the cubic close-packed (ccp) structure, with face-center cubic (fcc) unit cells. However, the difference in energy for the rare gas crystals between fcc and hexagonal close-packed (hcp) structure was estimated by Meyer[19] to be at most 0.1% of the lattice energy. Near the melting point the difference in energy between fcc and hcp was, as Meyer pointed out, at most of the order of 1% of the sublimation energy.

Barrett and Meyer also studied the structures and phase diagrams of Ar crystals containing N_2,[20] CO,[21] and O_2,[22] and found stable hcp structures over wide ranges of the impurity composition. Although pure N_2 and pure CO crystallize in hcp forms, the high temperature (γ) phase of O_2 is cubic and the addition of no more than 1% of O_2 to fcc Ar produced a stable hcp structure. Furthermore, in all three cases the temperature-composition line of the hcp-ccp transformation, when extrapolated to pure Ar, led Barrett and Meyer to conclude that Ar should be stable in the hcp form at higher temperatures with the hypothetical equilibrium temperature between hcp and fcc being a few degrees above the melting point.

The work of Curzon and Mascall[23] on pure Ar and pure Kr films deposited at 7°K showed only one fcc phase. This indicated that the mobilities of Ar and Kr at 7°K were high enough to give a well ordered crystal, at least on a microscopic scale. The work in paper I also indicated high mobilities of rare gas atoms around the trapped Pb atoms.

Because this allowed equilibrium state to be achieved, the possibility always remained that the matrices could have hcp structures around the trapped species.

The hcp structure differs from the fcc structure only in the number and distances of the third nearest neighbors and beyond; the potential constants of Lennard-Jones 6-12 equation for the two structures therefore are very nearly the same.[24] For the $^3P_1 \leftarrow {}^3P_0$ transition of Pb the upper state (7s orbital) is spherically symmetric and is only sensitive to the distances from the interacting atoms. Therefore, the earlier calculations for this transition were valid for both fcc and hcp structures.

As was mentioned, the ccp structure has a fcc unit cell and possesses cubic symmetry. The layer of atoms deposited parallel to the target surfaces constitute the [111] planes of the fcc crystal.[25] The p orbitals of the trapped species in a substitutional site of ccp crystals is therefore three-fold degenerate.

The earlier discussion indicated that penetration of metal atoms was expected toward inner layer matrix gas atoms. The penetration would be along the [111] axis, and would destroy the cubic symmetry of its interactions with the environment. However, it is easily seen that such penetration along the [111] axis would leave the three-fold degeneracy of the p orbitals unchanged. One of the two lobes of each p orbital is distorted while the other lobe is less distorted than before. The same occurs for all three p orbitals. The penetration might be slightly off from the [111] axis, but randomly; this could only broaden the spectral lines observed without causing splittings. The only effect of the metal

penetration would be to create a net asymmetric field along the [111] axis which might be interesting in the Stark splitting considered later.

Next, let us consider the metal atom in a hcp matrix film. As Fig. 3 shows, a metal atom at the substitutional site of a hcp lattice cannot maintain its three-fold degeneracy of the p orbitals. We are mainly interested in the difference in interactions between the metal and its nearest neighbors along x and y directions. The p orbitals of M, as Fig. 3 shows, do not interact the same in the x and y directions. As the orbital size becomes large, the overlap will set in with the neighbors on x axis while being less so in the y axis. The coordinate can be rotated as one wishes, but the interactions along any two mutually perpendicular axes in the x and y plane are not the same. When penetration along inner z axis is taken into account, the interaction with the inner neighbors due largely to the repulsive interaction will always make the interaction along the z axis the largest of the three. When the matrix film was warmed up, the whole film expanded outward from the target surface and increased the distortion between the p_z orbital and the inner matrix atoms. Expansion along the x and y axes, however, relieved the repulsion. This explained why it was always the absorption line highest in frequency that shifted to the blue when the film was warmed up, and the two lower frequency components to the red. For the Pb $^3P_1 \leftarrow {}^3P_0$ transition the upper state consisted of one 7s electron and one 6p electron. As was mentioned, only one line was expected because of the spherical symmetric nature of the 7s orbital. There was distortion of the inner layer matrix atoms due to -z penetration. The repulsive interaction due

to this distortion was expected to increase from Xe to Kr to Ar. In fact, the repulsive interaction in Ar could be so large that the frequency shift in Ar deviated by a large amount from the value based on a perfect substitutional site geometry. The earlier calculations indicated that the predicted shift in Ar was larger than that in Kr by 1100 cm^{-1}, if only the size effect was taken into account for a Pb atom in a substitutional site. However, the observed value was even larger than the predicted one by 1600 cm^{-1} which could not be explained by merely considering the size effect between Kr and Ar lattices, but could be explained at least qualitatively using the model proposed here.

In addition, this model predicted increasing distortion from the inner layer on warming up the matrix, which offset some of the relaxation effect along the x and y axes. The increase in distortion was expected to be largest in Ar, less in Kr and least in Xe. This might explain the increasing negative deviation observed in Kr matrix at higher temperatures than the calculated values. The deviation in Xe was, however, much less. Therefore, within the accuracies of the experimental measurements and the calculations shown in this work, the different deviations in Xe and Kr between the calculated and the observed frequency shifts at higher temperatures could be explained using our proposed model.

The case of Pb/Ar was interesting in that the observed blue shift from gas was much larger than was predicted and yet the red shift of this line on warming the Ar matrix was not proportionally large, as one would expect if the large $\Delta\nu$ came from equal contribution from all x, y and z axes due to distortions. Again, the model proposed could be used

to explain the abnormally large $\Delta\nu$ and the relatively small red shift on warming the Ar matrix.

The above discussion on hcp trapping sites also implies that for $p \leftarrow s$ transitions the larger the trapped metal p orbitals involved, the larger the observed frequency difference between transitions to p_x and p_y, and the smaller the difference between transitions to p_x and p_z orbitals. Let the observed triplets of those metals be denoted as ν_1, ν_2, and ν_3 in increasing frequency order, and corresponded to the transitions involving p_y, p_x and p_z orbitals, respectively, referring to Fig. 3. If $\Delta_{1,2}$ is for the difference in frequency between ν_1 and ν_2, etc., this model predicts that for a large trapped atom, or atoms with large increase of orbital size in the transition, $\Delta_{1,2} > \Delta_{2,3}$; and this difference decreases from Ar to Kr to Xe. The experimental observations from various literature are shown in Table IV.

The observed changes in $\Delta_{1,2}$ and $\Delta_{2,3}$, except for Ca and partly K, follow exactly as was predicted using the above model. These facts therefore support the possibility of having hcp structure in the matrices. X-ray work on the matrix structures is therefore very urgent in confirming this proposal.

Another interesting case is the large splitting in Au. Referring to Table V, the calculations[26] showed that much better agreement with experiment was obtained if all three lines were assigned to the same transition, i.e., $^2P_{\frac{1}{2}} \leftarrow {}^2S_{\frac{1}{2}}$, rather than using the assignment[2] of Morelle or King. Similar assignment was made to Ag and Cu. Under the new assignment, one must account for blue shifts of several thousand cm^{-1}

in Au, which are rather large shifts. The earlier work on Pb showed that large energy shifts could be expected. If the predicted hcp structure is proved to be true, the larger orbital expansion of Au during the excitation would give a large distortion on the p_x orbital which could approximate in energy that of p_z; the latter suffered large distortion from the inner layer matrix atoms due to the metal penetration. Reliable calculations are needed to confirm this. The Lennard-Jones potential was shown to be unsuitable for interactions involving strong overlap with the p orbitals. Quantum mechanical calculations are needed to properly take into consideration the orientation effect and the correct trapping site geometry. What has been shown in this work is that at least qualitatively the large splitting in those atoms can be expected, in addition to the successful interpretation of many other experimental facts using our proposed model.

Conclusions

A method was demonstrated to predict the gas phase transition frequency using the line frequencies observed in Xe and Kr matrices. This is helpful in identifying the absorbing species in the gas by locating its resonance transition in the gas phase spectrum using the data in the matrices.

The results of this work showed that this method worked well for the metal atoms with $s \leftarrow p$ resonance transitions, but not so for the metal atoms with $p \leftarrow s$ resonance transitions. This is explained as due

to the validity of using the Lennard-Jones potential calculation in the former case but not in the latter. The work indicated that if one observed a single, strong absorption line in Xe and Kr matrices, which shifted to lower frequencies on warming the matrices, one might approximate with some confidence the gas phase ν° of this transition using the method shown in this work. On the other hand, when multiplet lines were observed, one should be cautious in doing so, and should keep in mind that the calculated ν_{gas} was lower than the true ν_{gas}. It is hoped, however, that this calculated value can sometimes be used as the lower limit of the true ν_{gas} and offer some helpful information.

A model was proposed to account for both the static and dynamic matrix effects observed in the matrices. The proposed model was partly based on an assumed hcp structure of the trapping site in the matrices which was based on various indirect experimental observations. Direct structure determination is needed to confirm it. However, this work clearly indicated that the trapping site geometry must be playing a central role in the observed static and dynamic matrix effects on the trapped atomic spectra in the matrices.

Acknowledgments

The author wishes to thank Professor Leo Brewer for his guidance and suggestions in this work. This work was performed under the auspices of the U. S. Atomic Energy Commission.

Appendix: Stark Effect in the Matrices

When an electric field E is applied to an atom with an electric moment $\vec{P}$ the Hamiltonian for the atom in the applied field is

$$H = H_o - \vec{E} \cdot \vec{P}$$

where H_o is the unperturbed Hamiltonian. Therefore, the change of energy levels is governed by the matrix components of $\vec{P}$. From the second-order perturbation theory, the shift of an energy state, in an electric field, due to the coupling with another state allowed by the selection rules is

$$| < A \; |E \; P| \; B > |^2 / \; |W_A - W_B| \qquad (1)$$

Here W_A and W_B are the unperturbed energies of states A and B, respectively. The matrix $| < A \; |E \; P| \; B > |$ has the value of the order $6.4 \; n^2 \; cm^{-1}$ for a field of 10^5 volt/cm, n being the principal quantum number.[27] Because of the selection rules different sublevels of an energy state usually are perturbed to different extents by the neighboring energy levels. The differences in the energy shift among the sublevels then give the splitting energies observed.

The energy shift one would expect in a matrix field is now approximated. Take Pb for example; calculations[26] showed that the interaction energy of Pb and Xe at the normal distance of separation in a matrix was about 10^3 $cm^{-1}/3.90$ Å. This is of the order of 10^6 volt/cm. The expected shift in energy for Pb was therefore calculated to be about 150 cm^{-1} for an energy difference of 35 000 cm^{-1} between the two states.

For the other metals like Au, their interactions with Xe and Kr were larger than those for Pb.[26] A splitting of several hundred cm^{-1} from the $^2P_{\frac{3}{2}}$ state is therefore expected. The field strength used here is the interaction energy of a Xe-Pb pair or a Xe-Au pair. This is about what one would expect when the metal penetration toward inner layer matrix atoms is taken into account.

In most cases, in addition to the splittings observed all the triplet components of the trapped metals shifted from the gas phase absorption frequencies. This can be explained on the basis of calculations for the Pb frequencies. There the shift was mainly due to the difference in the interactions of the ground and excited states of Pb with the surrounding matrix atoms. Such shift still existed even for a Pb atom in a perfect substitutional site. Further splitting of the sublevels of metals with $p \leftarrow s$ transitions came in only when there was a net asymmetric field in the matrix, cuased by distortion, for example. In this way, one explained, within the framework of Stark splitting discussions, the observed shift and splitting of the multiplet components in the matrices.

Now let us consider the dynamic matrix effect predicted by the Stark splitting model. With the Stark effect, the $^2P_{\frac{3}{2}}$ state of Au, Ag, Cu and alkali metals are split into two substrates with $M_J = \pm \frac{3}{2}$ and $\pm \frac{1}{2}$, respectively. According to the Stark splitting theory both substates are shifted to the same direction with increasing strength of the electric field. The local field strength at a trapped atom changes on warming the matrix; this implies that the transitions to these two states should shift to the same direction with increasing matrix

temperatures. Another effect on the absorption frequencies upon warming the matrix is the decreasing interaction between the metal and the matrix atoms. The sum of these two effects again would in most cases predict that the two components of the $^2P_{\frac{3}{2}}$ state shift to the same direction. This is in clear contradiction with experiment.

Next, with a Stark effect the $^2P_{\frac{1}{2}}$ state gives only one component with $M_J = \pm \frac{1}{2}$. This state should behave very similarly to the $M_J = \pm \frac{1}{2}$ component from the $^2P_{\frac{3}{2}}$ state. The latter should be lower in energy than the component with $M_J = \pm \frac{3}{2}$ because, taking Ag for an example, the perturbations from the higher levels are larger than those from the lower levels due to the closer spacing in energies in the former. All the higher states having substates with $J = \frac{3}{2}$ also have $J = \frac{1}{2}$ substrates, but the reverse is not necessarily true. This means every state which perturbs the $M_J = \pm \frac{3}{2}$ level also perturbs the $M_J = \pm \frac{1}{2}$ level but not the reverse way. The $M_J = \pm \frac{1}{2}$ level is therefore pushed down more than the $M_J = \pm \frac{3}{2}$ level. From Eq. 1 one notices that as $\Delta E(^2P_{\frac{1}{2}} \leftarrow {}^2P_{\frac{3}{2}})$ approaches zero, so is the difference in energy between the two levels with $M_J = \pm \frac{1}{2}$. Again the triplet components are labelled as ν_1, ν_2, and ν_3 in increasing energy order, and correspond to the components $^2P_{\frac{1}{2}}$ $(M_J = \pm \frac{1}{2})$, $^2P_{\frac{3}{2}}$ $(M_J = \pm \frac{1}{2})$ and $^2P_{\frac{3}{2}}$ $(M_J = \pm \frac{3}{2})$, respectively. When ΔE $(^2P_{\frac{1}{2}} \rightarrow {}^2P_{\frac{3}{2}})$ is not too large $(\nu_2 - \nu_1)$ should approach ΔE, and should be quite independent of the field change from Xe to Kr. The latter should be a more reliable criterion because the former depends on the relative importance of ΔE to $(W_A - W_B)$ in the calculations using Eq. 1.

However, after taking this correction into account the criterion that $(\nu_2 - \nu_1)$ be matrix gas independent should be more rigorous.

From Table V one notices that this is not what was observed. The change for $(\nu_2 - \nu_1)$ in going from Xe to Kr matrices was rather large for the metals, being 700, 230 and 130 cm^{-1} in Au, Ag and Cu, respectively. Furthermore, it is interesting to notice the rather small change in $(\nu_3 - \nu_2)$ which was 98, 12 and 30 cm^{-1} in Au, Ag and Cu, respectively. The small $(\nu_3 - \nu_2)$ change between Xe and Kr matrices is again in contrast to what would be predicted by the Stark theory. The field was expected to change quite significantly from Xe to Kr; this would cause large changes in the splitting energy for the $\pm \frac{3}{2}$ and $\pm \frac{1}{2}$ substates from the same $^2P_{\frac{3}{2}}$ state.

References

1. L. Brewer and C-A Chang, J. Chem. Phys., manuscript submitted for publication; hereafter referred to as paper I.
2. B. Meyer, Low Temperature Spectroscopy; Optical Properties of Molecules in Matrices, Mixed Crystals and Glasses, American Elsevier, New York, 1971.
3. L. Andrews and G.C. Pimentel, J. Chem. Phys. 47, 2905 (1967).
4. B. Meyer, J. Chem. Phys. 43, 2986 (1965).
5. L. Brewer, B.A. King, J.L. Wang, B. Meyer and G.F. Moore, J. Chem. Phys. 49, 5209 (1968).
6. J.L. Wang, Ph.D. Thesis, University of California, Berkeley, UCRL-19093, 1969.
7. M. McCarty, Jr. and G. W. Robinson, Mol. Phys. 2, 415 (1959).
8. M. Brith and O. Schnepp, J. Chem. Phys. 39, 2714 (1963).
9. L. Brewer and B. A. King, J. Chem. Phys. 53, 3981 (1970).
10. B. A. King, Ph.D. Thesis, University of California, Berkeley, UCRL-18618, 1968.
11. M. McCarty, Jr., J. Chem. Phys. 52, 4973 (1970).
12. G. L. Pollack, Rev. Mod. Phys. 36, 748 (1964).
13. D. L. Losee and R. O. Simmons, Phys. Rev. 172, 944 (1968).
14. H. Margenau and W. W. Watson, Rev. Mod. Phys. 8, 22 (1936); S. Ch'en and T. Takeo, Rev. Mod. Phys. 29, 20 (1957); M. B. Robin and N. A. Kuebler, J. Mol. Spectrosc. 33, 274 (1970).
15. W. W. Duley, Ph.D. Thesis, Imperial College, London, 1966.
16. W. Weyhmann and F. M. Pipkin, Phys. Rev. 137A, 490 (1965).
17. G. C. Pimentel in "Formation and Trapping of Free Radicals", H.P. Broida and A. M. Bass, Eds., Academic Press Inc., 1960, Chapter 4.
18. K. Chopra, "Thin Film Phenomena", McGraw Hill Inc., New York, 1969.
19. L. Meyer, Adv. in Chem. Phys., Vol. XV, 343 (1969).
20. C. S.Barrett and L. Meyer, J. Chem. Phys. 42, 107 (1965).
21. C. S. Barrett and L. Meyer, J.Chem. Phys. 43, 3502 (1965).

22. C. S. Barrett, L. Meyer and J. Wasserman, J. Chem. Phys. 44, 998 (1966).
23. A. E. Curzon and A. J. Mascall, J. Phys., C (Solid State Phys.), 220, Ser. 2, Vol. 2, (1969).
24. T. Kihara and S. Koba, J. Phys. Soc. Japan 7, 348 (1952).
25. L. Pauling, "Nature of the Chemical Bond," Cornell University Press, N.Y. 1960, 3rd Ed., p. 406.
26. C-A Chang, Ph.D. Thesis, University of California, Berkeley, UCRL-19662, 1970.
27. E. U. Condon and G. H. Shortley, "The Theory of Atomic Spectra," Cambridge University Press, 1935, Chapter XVII.

TABLE I. Calculated and observed warm-up shifts of the Pb $^3P_1 \leftarrow {}^3P_0$ line in Xe and Kr matrices.

	Temperature (°K)	d_{ab}(Å)	$\Delta\nu^{calc}$ cm^{-1}	$\Delta\nu^{obs}$ cm^{-1}
Xe	20	4.34	2483	2483
	30	4.345	2451	2437
	40	4.352	2408	2379
	50	4.361	2355	2317
	60	4.371	2296	2260
	70	4.380	2245	2210
	77	4.389	2196	2148
Kr	20	3.999	2974	2974
	30	4.005	2930	2928
	40	4.014	2860	2896
	50	4.025	2771	2858

TABLE II. Calculated and observed warm-up shifts of the Pb $^3P_1 \leftarrow {}^3P_0$ line in the 10% Xe - 90% Kr matrix.

Temperature (°K)	$\Delta\nu^{calc*}$ cm^{-1}	$\Delta\nu^{obs*}$ cm^{-1}	$\Delta\nu^{obs‡}$ cm^{-1}
20	2646	2659	2659
30	2601	2590	2598
40	2551	2551	2532
50	2498	2492	2492

* The values from the corresponding ones in the Xe and Kr matrices from Table I, using the approximation that

$$\Delta\nu_{Xe\text{-}Kr} \approx \frac{8}{12}\Delta\nu_{Xe} + \frac{4}{12}\Delta\nu_{Kr} .$$

‡ The experimental values.

TABLE III. Calculated ν_{gas} values of the various metals

Metal	ν(M/Xe)cm^{-1}	ν(M/Kr)cm^{-1}	ν_{gas}^{calc} cm^{-1}	$\nu_{gas}^{expt.}$ cm^{-1}
Pb	37 770	38 261	35 290	35 287($6p7s\ ^3P_1 \leftarrow 6p^2\ ^3P_0$)
Bi	35 971	36 363	33 900	32 605 ($6p^2 7s\ ^4S_{\frac{1}{2}} \leftarrow 6p^3\ ^4S_{\frac{3}{2}}$)
Au	36 860	38 300	30 360	37 359 ($^2P_{\frac{1}{2}} \leftarrow {}^2S_{\frac{1}{2}}$)
	40 355	42 499	30 880	41 174 ($^2P_{\frac{3}{2}} \leftarrow {}^2S_{\frac{1}{2}}$)
	40 969	43 011	31 920	
Ag	29 886	30 989	24 810	29 552 ($^2P_{\frac{1}{2}} \leftarrow {}^2S_{\frac{1}{2}}$)
	30 553	31 888	24 490	30 473 ($^2P_{\frac{3}{2}} \leftarrow {}^2S_{\frac{1}{2}}$)
	30 998	32 321	24 990	
Cu	30 647	31 766	25 500	30 535 ($^2P_{\frac{1}{2}} \leftarrow {}^2S_{\frac{1}{2}}$)
	30 893	32 144	25 190	30 783 ($^2P_{\frac{3}{2}} \leftarrow {}^2S_{\frac{1}{2}}$)
	31 240	32 520	25 410	
K	12 424	12 623	11 170	12 989 ($^2P_{\frac{1}{2}} \leftarrow {}^2S_{\frac{1}{2}}$)
	12 687	12 938	11 210	13 047 ($^2P_{\frac{3}{2}} \leftarrow {}^2S_{\frac{1}{2}}$)
	12 952	13 215	11 430	
Cs	10 807	11 036	9 420	11 181 ($^2P_{\frac{1}{2}} \leftarrow {}^2S_{\frac{1}{2}}$)
	11 240	11 533	9 590	11 736 ($^2P_{\frac{3}{2}} \leftarrow {}^2S_{\frac{1}{2}}$)
	11 643	11 936	9 990	

TABLE IV. Triplet splitting for atoms in matrices.

Metal[†]	Observed differences between $\Delta_{1,2}$ and $\Delta_{2,3}$	Dependence of $(\Delta_{1,2} - \Delta_{2,3})$ on matrix gas
Li, Na, K*, Rb	$\Delta_{1,2} < \Delta_{2,3}$	not reported
Cs	$\Delta_{1,2} > \Delta_{2,3}$	in Ar > in Kr > in Xe
Au	$\Delta_{1,2} > \Delta_{2,3}$	in Kr > in Xe
Ag	$\Delta_{1,2} > \Delta_{2,3}$	in Ar > in Kr > in Xe
Cu	$\Delta_{1,2} < \Delta_{2,3}$ in Xe but $\Delta_{1,2} \sim \Delta_{2,3}$ in Kr	
Mg[‡]	$\Delta_{1,2} > \Delta_{2,3}$	in Kr > in Xe

[†] Metals in the same series should be compared to eliminate complexities other than the orbital size change and interactions involved.

* K does not follow this trend too well.

[‡] Ca shows just the opposite with $\Delta_{1,2} < \Delta_{2,3}$ in Kr and $\Delta_{1,2} > \Delta_{2,3}$ in Xe.

TABLE V. Absorption spectra of gold in the matrices by King[9,10]

Matrix	$\nu(cm^{-1})$	Assignment	Gas Phase Frequency (cm^{-1})	$\nu-\nu_o(cm^{-1})$
Xe	36 860	$^2P_{\frac{1}{2}} \leftarrow {}^2S_{\frac{1}{2}}$	(37 359)	-499
	40 355	$^2P_{\frac{3}{2}} \leftarrow {}^2S_{\frac{1}{2}}$	(41 174)	-819
	40 969			-205
Kr	38 300	$^2P_{\frac{1}{2}} \leftarrow {}^2S_{\frac{1}{2}}$	(37 359)	+941
	42 499	$^2P_{\frac{3}{2}} \leftarrow {}^2S_{\frac{1}{2}}$	(41 174)	+1325
	43 011			+1837

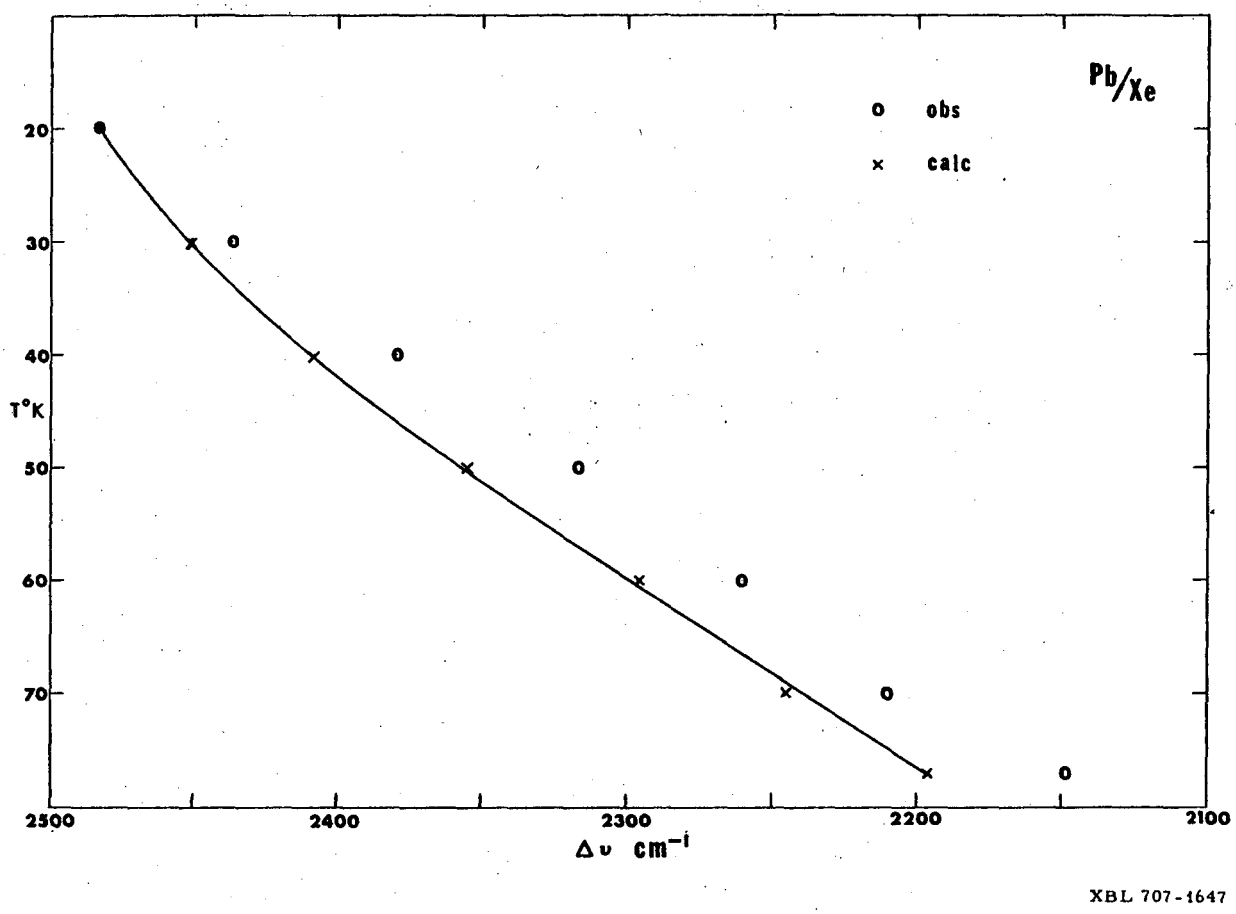

Fig. 1 Calculated and observed warm-up shifts of Pb/Xe.

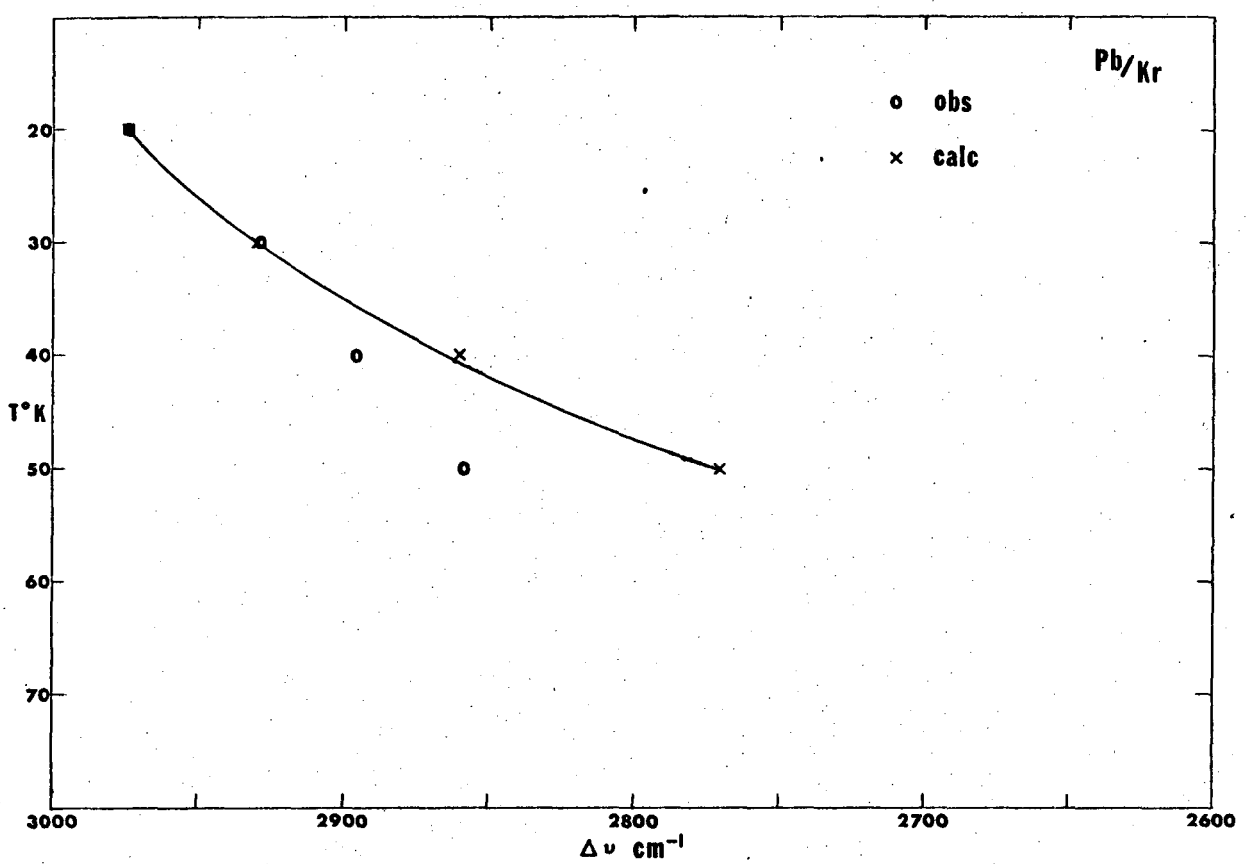

Fig. 2 Calculated and observed warm-up shifts of Pb/Kr.

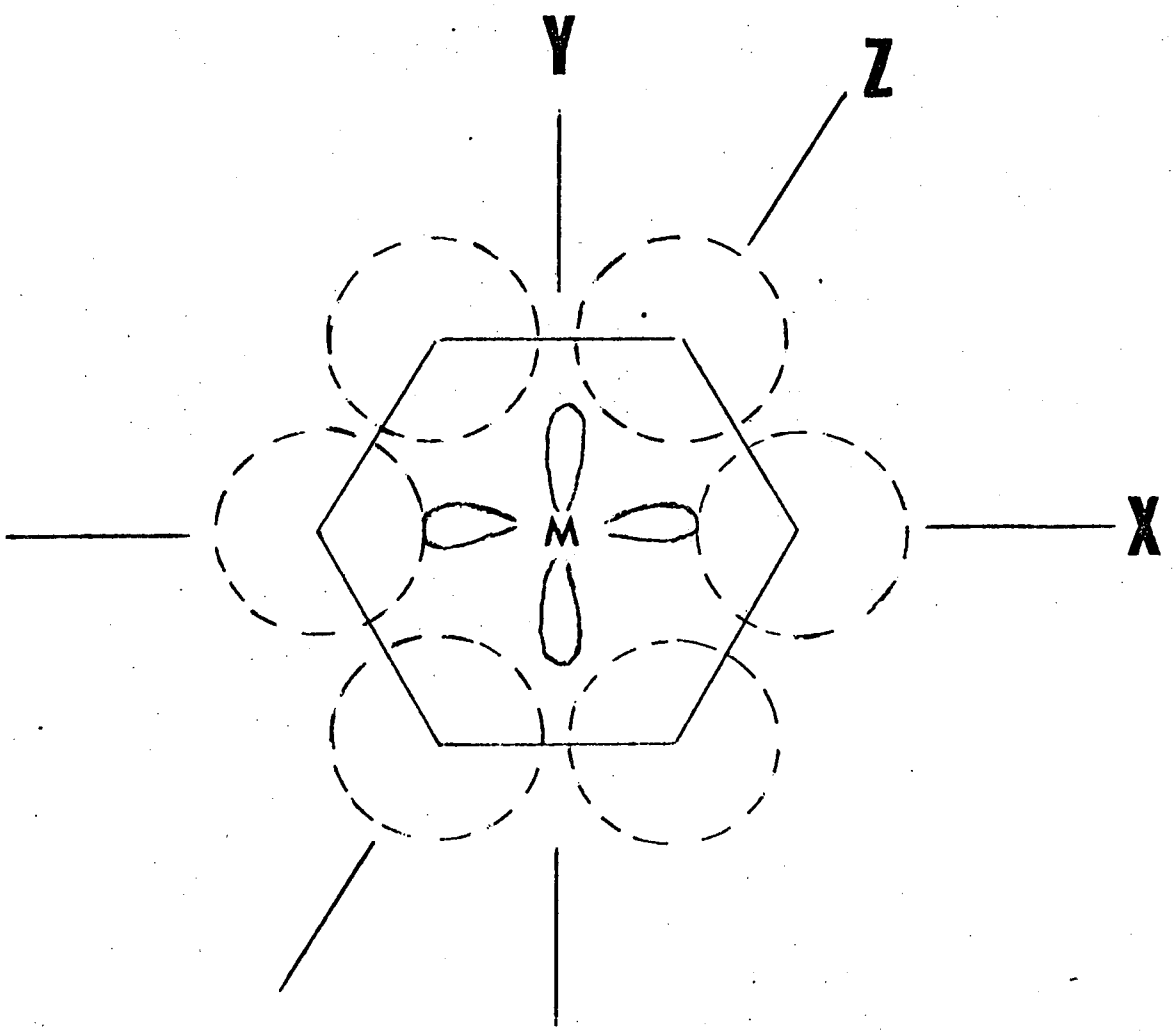

XBL 707-1588

Fig. 3 The metal p orbitals in a hcp matrix gas lattice.

TECHNICAL INFORMATION DIVISION
LAWRENCE BERKELEY LABORATORY
UNIVERSITY OF CALIFORNIA
BERKELEY, CALIFORNIA 94720